

**A NOTE ON SCATTERING OF RAYLEIGH WAVES  
BY SHALLOW CIRCULAR CANYONS: ANALYTICAL APPROACH**

by

**M.I. Todorovska<sup>1)</sup> and V.W. Lee<sup>2)</sup>**

*Dept. of Civil Engineering, University of Southern California  
Los Angeles, CA 90089-8591*

**ABSTRACT**

An analytical method has been developed to study the steady-state diffraction and scattering of mono-chromatic Rayleigh waves by shallow circular canyons. The shape of the canyon can vary from very shallow to semi-circular. The method is based on representation of the scattered waves in series of cylindrical wave functions and on approximation of the half-space surface by a cylindrical surface of very large radius. Along the canyon bottom the stresses of the free-field motion are approximated by finite Fourier series to satisfy the zero-stress boundary condition there. The horizontal and vertical displacement amplitudes are illustrated for canyon motion excited by Rayleigh waves with different wave lengths.

**INTRODUCTION**

The strong earthquake ground motion can be changed significantly by the irregular surface topography. When the size of the irregularities is comparable to or larger than the wave lengths of the incident waves diffraction and scattering take place, resulting in amplification and spatial variation of the incident motion close to the irregularities. In earthquake engineering and strong motion seismology numerical methods such as finite elements, finite differences, boundary integral equation and the method of line sources have been employed to study these phenomena. (Wong, 1987; Sánchez-Sesma, 1979; and many others). On the other hand only a small number of analytical methods have been

---

<sup>1)</sup> Research Associate  
<sup>2)</sup> Associate Professor

presented. For the scattering and diffractions of plane SH waves from semi-circular and semi-elliptical canyons (Trifunac, 1973; Wong and Trifunac, 1974) in two-dimensional half-space and for a semi-spherical canyon (Lee, 1982) in the three-dimensional half-space. Recently, an approximate analytical method was developed by Cao and Lee (1989, 1990) and Lee and Cao (1989) for scattering of plane SH, P and SV waves from shallow circular canyons (depth-to-half-width ratio  $\leq 1$ ).

The purpose of this paper is to extend the method of Lee and Cao (1989) to shallow canyons for incident monochromatic Rayleigh waves. Since a large portion of the destructive seismic energy is transmitted to the sites of important structures via surface waves (Trifunac, 1971), the application of their method to this type of excitation is a useful extension of their work. The purpose of this paper is also to discuss this analytical method and to illustrate some results that may help understand the physical phenomena associated with this problem.

Dynamic response of long structures (dams, bridges) supported by canyon walls, which move with different amplitudes and out of phase is affected profoundly by the physical nature of scattering and diffraction of strong motion near structural foundations. This was studied by Kojić et al. (1988) for concrete arch dams. They showed that the out of phase motions of the canyon walls can produce excessive stresses and that such excitations must be considered in any major analysis of long earthquake resistant structures. To this end, this paper represents a contribution to future improvement of our capabilities to compute the realistic excitation of such long structures. Once the method has been fully developed and tested it can easily be generalised to irregular shapes of the canyon walls (Moeen-Vasiri and Trifunac, 1988a,b).

### THE MODEL

The model studied here consists of a two-dimensional homogeneous and isotropic half-space with a circular canyon (Fig. 1). The center and radius of curvature of the canyon are at  $O_1$  and  $b$ , respectively, and  $d$  is the distance from  $O$ , to the half-space surface. The shear wave velocity, shear modulus and Poisson's ratio of the half-space are  $\beta$ ,  $\mu$  and  $\nu$ . The rectangular coordinate systems  $x - O - x$ ,  $x_1 - O_1 - x_1$  and  $x_2 - O_2 - x_2$  and the polar

coordinate systems  $r_1 - \theta_1$  and  $r_2 - \theta_2$  are used to describe the geometry and to express the excitation and the scattered waves. The distance between the origins of the two polar coordinate systems is  $D$ .

The in-plane disturbances in the elastic half-space can be described by the potentials  $\phi$  and  $\psi$  of the  $P$  and  $S$  waves, respectively. These have to satisfy the corresponding two-dimensional wave equations, that in the  $r_1 - \theta_1$  coordinate system have the following form:

$$\left( \frac{\partial^2}{\partial r_1^2} + \frac{1}{r_1} \frac{\partial}{\partial r_1} + \frac{1}{r_1^2} \frac{\partial^2}{\partial \theta_1^2} \right) \phi = \frac{1}{\alpha^2} \frac{\partial^2 \phi}{\partial t^2} \quad (1a)$$

and

$$\left( \frac{\partial^2}{\partial r_1^2} + \frac{1}{r_1} \frac{\partial}{\partial r_1} + \frac{1}{r_1^2} \frac{\partial^2}{\partial \theta_1^2} \right) \psi = \frac{1}{\beta^2} \frac{\partial^2 \psi}{\partial t^2} \quad (1b)$$

where  $\alpha = \sqrt{2(1-\nu)/(1-2\nu)}\beta$  is the P-wave velocity in the half-space. In steady-state, the motion in the half-space can be calculated by superimposing the scattered waves to the free-field motion, all together satisfying the prescribed boundary conditions. Those conditions are

$$\begin{pmatrix} \tau_{zz} \\ \tau_{zx} \end{pmatrix} = \begin{pmatrix} 0 \\ 0 \end{pmatrix} \text{ at } z = 0 \quad (2a)$$

and

$$\begin{pmatrix} \tau_{r_1 r_1} \\ \tau_{r_1 \theta_1} \end{pmatrix} = \begin{pmatrix} 0 \\ 0 \end{pmatrix} \text{ at } r_1 = b \quad (2b)$$

where  $\tau_{zz}$ ,  $\tau_{zx}$ ,  $\tau_{r_1 r_1}$  and  $\tau_{r_1 \theta_1}$  are the stress components in the half-space. The displacement components  $u_x$  and  $u_z$ , in the  $x$  and in the  $z$  directions, respectively, and  $u_{r_1}$  and  $u_{\theta_1}$ , in the  $r_1$  and  $\theta_1$  directions, can be calculated from the potentials as follows:

$$u_x = \frac{\partial \phi}{\partial x} - \frac{\partial \psi}{\partial z} \quad (3a)$$

$$u_z = \frac{\partial \phi}{\partial z} + \frac{\partial \psi}{\partial x} \quad (3b)$$

$$u_{r_1} = \frac{\partial \phi}{\partial r_1} + \frac{1}{r_1} \frac{\partial \psi}{\partial \theta_1} \quad (3c)$$

and

$$u_{\theta_1} = \frac{1}{r} \frac{\partial \phi}{\partial \theta_1} - \frac{\partial \psi}{\partial r_1} \quad (3d)$$

The stresses then can be calculated by differentiation of the displacements, i.e.

$$\tau_{zz} = \lambda \left( \frac{\partial u_x}{\partial x} + \frac{\partial u_z}{\partial z} \right) + 2\mu \frac{\partial u_z}{\partial z} \quad (4a)$$

$$\tau_{zx} = \mu \left( \frac{\partial u_x}{\partial z} + \frac{\partial u_z}{\partial x} \right) \quad (4b)$$

$$\tau_{r_1 r_1} = \lambda \left( \frac{\partial u_{r_1}}{\partial r_1} + \frac{u_{r_1}}{r_1} + \frac{1}{r} \frac{\partial u_{\theta_1}}{\partial \theta_1} \right) + 2\mu \frac{\partial u_{r_1}}{\partial r_1} \quad (4c)$$

and

$$\tau_{r_1 \theta_1} = \mu \left( \frac{\partial u_{\theta_1}}{\partial r_1} - \frac{u_{\theta_1}}{r_1} + \frac{1}{r_1} \frac{\partial u_{r_1}}{\partial \theta_1} \right) \quad (4d)$$

where  $\lambda$  is the Lamé constant.

### The Far-field Motion

A monochromatic Rayleigh wave can be represented through its potentials as follows

$$\phi = C e^{-b_1 z} e^{ik(x-ct)} \quad (5a)$$

$$\psi = D e^{-b_2 z} e^{ik(x-ct)} \quad (5b)$$

where  $C$  and  $D$  are complex constants,  $b_1$  and  $b_2$  are real and positive constants and  $k$  and  $c$ , both real, are the wave number and the phase velocity of the surface waves propagating in the positive  $x$ -direction. These constants are related as follows

$$b_1 = k\sqrt{1 - (c/\alpha)^2} \quad (6a)$$

$$b_2 = k\sqrt{1 - (c/\beta)^2} \quad (6b)$$

and

$$D = \frac{1}{2b_2 ik} (k^2 + b_2^2) C \quad (7)$$

(Eringen and Şuhubi, 1975). The eigenvalues of the phase velocity  $c$  satisfy the Rayleigh equation and have values e.g.  $c = 0.9194\beta$  for  $\nu = 1/4$  and  $c = 0.9320$  for  $\nu = 1/3$ . The particle motion is elliptical retrograde up to certain depth and then the direction of rotation changes.

It is convenient to introduce complex angles  $\theta_\alpha$  and  $\theta_\beta$  defined as follows

$$\theta_\alpha = \frac{\pi}{2} - i\phi_\alpha \quad (8a)$$

$$\theta_\beta = \frac{\pi}{2} - i\phi_\beta \quad (8b)$$

where  $\phi_\alpha$  and  $\phi_\beta$  are real quantities such that

$$\cosh \phi_\alpha = \alpha/c \quad (8c)$$

$$\cosh \phi_\beta = \beta/c. \quad (8d)$$

In terms of those angles

$$\phi = C e^{b_1 d} e^{i k_\alpha r_1 \cos(\theta_1 - \theta_\alpha) - i \omega t} \quad (9a)$$

and

$$\psi = D e^{b_2 d} e^{i k_\beta r_1 \cos(\theta_1 - \theta_\beta) - i \omega t} \quad (9b)$$

where  $k_\alpha = \omega/\alpha$  and  $k_\beta = \omega/\beta$  are the wave numbers of the *P* and *S* waves in the half-space, and  $\omega$  is the circular frequency.

### The Scattered Waves

The scattered waves will be defined in terms of their *P* and *S*-potentials, which can be represented by Bessel-Fourier series as follows:

$$\phi^R = \phi_1^R + \phi_2^R \quad (10a)$$

and

$$\psi^R = \psi_1^R + \psi_2^R \quad (10b)$$

where

$$\phi_1^R = \phi_1^R(r_1, \theta_1, t) = \sum_{n=0}^{\infty} H_n^{(1)}(k_\alpha r_1) \left( A_{1,n}^R \cos n\theta_1 + B_{1,n}^R \sin n\theta_1 \right) e^{-i\omega t} \quad (11a)$$

$$\psi_1^R = \psi_1^R(r_1, \theta_1, t) = \sum_{n=0}^{\infty} H_n^{(1)}(k_\beta r_1) \left( C_{1,n}^R \sin n\theta_1 + D_{1,n}^R \cos n\theta_1 \right) e^{-i\omega t} \quad (11b)$$

$$\phi_2^R = \phi_2^R(r_2, \theta_2, t) = \sum_{n=0}^{\infty} J_n(k_\alpha r_2) \left( A_{2,n}^R \cos n\theta_2 + B_{2,n}^R \sin n\theta_2 \right) e^{-i\omega t} \quad (12a)$$

and

$$\psi_2^R = \psi_2^R(r_2, \theta_2, t) = \sum_{n=0}^{\infty} J_n(k_\beta r_2) \left( C_{2,n}^R \sin n\theta_2 + D_{2,n}^R \cos n\theta_2 \right) e^{-i\omega t}. \quad (12b)$$

$\phi_2^R$  and  $\psi_2^R$  can be transformed into Bessel-Fourier series in the  $r_1 - \theta_1$  coordinate system and relationships between the coefficients of those series and the coefficients of  $\phi_1^R$  and  $\psi_1^R$  can be established via the application of the addition theorem and the zero-stress condition on the surface the big circle (Cao and Lee, 1990).

#### Solution of the problem

To match the zero-stress condition at  $r_1 = b$  it is necessary first to transform the far-field motion into a form compatible with the representation of the scattered waves. Lee and Cao (1989) expanded the potential of the inhomogeneous P-wave of the far-field motion, for incidence beyond critical, at  $r_1 = b$  in finite Fourier series of  $\theta_1$ . To achieve convergence of the series they first modified the potential by assigning to it the value zero for  $s < 0$ . Todorovska and Lee (1991b) found it more appropriate to derive analytically the stresses and the displacements of the inhomogeneous P wave from its potential and then to expand those at  $r_1 = b$  in finite Fourier series of  $\theta_1$ . For the same reason, they also first modified the expressions for the stresses and the displacements by extending those into the region above the half-space symmetrically about  $\theta_1 = \pm\theta_0$ , where  $\theta_0 = \cos^{-1}(d/b)$ . Avoiding the jumps at  $\theta_1 = \pm\theta_0$ , their finite Fourier series had smaller oscillations and therefore better represented the quantities that they approximated.

In this paper the procedure of Todorovska and Lee (1991b) was followed. The stresses of the free-field motion,  $\tau_{r_1 r_1}^{f-f}$  and  $\tau_{r_1 \theta_1}^{f-f}$ , were derived from the potentials in equations (9a,b) by applying the expressions in equations (3c,d) and (4c,d) and then approximated by

$$\tau_{r_1 r_1}^{f-f}(b, \theta_1, t) \approx \frac{2\mu}{b^2} \sum_{n=0}^N \left( A_{0,n}^{r_r} \cos n\theta_1 + B_{0,n}^{r_r} \sin n\theta_1 \right) e^{-i\omega t} \quad (13a)$$

and

$$\tau_{r_1 \theta_1}^{f-f}(b, \theta_1, t) \approx \frac{2\mu}{b^2} \sum_{n=0}^N \left( A_{0,n}^{r_\theta} \cos n\theta_1 + B_{0,n}^{r_\theta} \sin n\theta_1 \right) e^{-i\omega t}. \quad (13b)$$

The stresses of the scattered waves were derived from their potentials following the same equations for the potential-displacement and displacement-stress relations.

The application of the zero-stress condition at  $r = b$ , equation (26), yields the following systems of equations, where the unknowns are the coefficients of the series expansions of

$\phi_1^R$  and  $\phi_2^R$ :

$$\sum_{j=0}^{\infty} \left\{ \Re[\mathcal{E}^{(s)}(n,b)] \begin{bmatrix} R_{nj}^+(k_\alpha^{(s)} D) & 0 \\ 0 & R_{nj}^-(k_\beta^{(s)} D) \end{bmatrix} - |\mathcal{E}^{(s)}(n,b)| \delta_{nj} \right\} \begin{pmatrix} A_{1,j}^R \\ C_{1,j}^R \end{pmatrix} = \begin{pmatrix} A_{0,n}^* \\ C_{0,n}^* \end{pmatrix} \quad n=0,1,2,\dots \quad (14a)$$

and

$$\sum_{j=0}^{\infty} \left\{ \Re[\mathcal{E}^{(s)}(n,b)] \begin{bmatrix} R_{nj}^-(k_\alpha^{(s)} D) & 0 \\ 0 & R_{nj}^+(k_\beta^{(s)} D) \end{bmatrix} - |\mathcal{E}^{(s)}(n,b)| \delta_{nj} \right\} \begin{pmatrix} B_{1,j}^R \\ D_{1,j}^R \end{pmatrix} = \begin{pmatrix} B_{0,n}^* \\ D_{0,n}^* \end{pmatrix} \quad n=0,1,2,\dots \quad (14b)$$

where

$$R_{nj}^\pm(kD) = \frac{\epsilon_n}{2} \sum_{i=0}^{\infty} \frac{\epsilon_i}{2} \left[ J_{n+i}(kD) \pm (-1)^i J_{n-i}(kD) \right] \left[ H_{i+j}(kD) \pm (-1)^j H_{i-j}(kD) \right] \quad (15)$$

$\Re$  stands for real part and  $[\mathcal{E}^{(s)}(n,r)]_{2 \times 2}$  has terms

$$\mathcal{E}_{11}^{(s)}(n,r) = (n^2 + n - \frac{1}{2} k_\alpha^2 r^2) H_n^{(1)}(k_\alpha r) - k_\alpha r H_{n-1}^{(1)}(k_\alpha r) \quad (16a)$$

$$\mathcal{E}_{12}^{(s)}(n,r) = \pm n \left[ -(n+1) H_n^{(1)}(k_\beta r) + k_\beta r H_{n-1}^{(1)}(k_\beta r) \right] \quad (16b)$$

$$\mathcal{E}_{21}^{(s)}(n,r) = \mp n \left[ -(n+1) H_n^{(1)}(k_\alpha r) + k_\alpha r H_{n-1}^{(1)}(k_\alpha r) \right] \quad (16c)$$

and

$$\mathcal{E}_{22}^{(s)}(n,r) = -(n^2 + n - \frac{1}{2} k_\beta^2 r^2) H_n^{(1)}(k_\beta r) + k_\beta r H_{n-1}^{(1)}(k_\beta r) . \quad (16d)$$

These infinite systems of equations are first truncated and then solved numerically. Once the coefficients  $\{A_{1,n}^R\}$ ,  $\{B_{1,n}^R\}$ ,  $\{C_{1,n}^R\}$  and  $\{D_{1,n}^R\}$  are known the coefficients of  $\phi_1^R$  and  $\phi_2^R$ , as well as the overall displacements of the scattered waves can be calculated. If desired, the response in the time domain can be calculated by the method of Fourier synthesis.

## RESULTS AND DISCUSSION

Figures 2 through 6 illustrate the displacement amplitudes and phases on the surface of the half-space and on the canyon bottom for incident Rayleigh waves with unit amplitude of the horizontal displacement component at  $z = 0$ . The Poisson's ratio is  $\nu = 1/3$  and for this value the ratio of the amplitudes of the displacement components of the free-field motion at  $z = 0$  is  $|u_x|/|u_z| = 1.56$ . The solid and the dashed lines are associated with the horizontal and the vertical displacement components, respectively. The phases have been shown so that at  $z = 0$  the phase is zero. In Fig. 2,3,4 and 5 the canyon is shallow

( $h/b = 0.5$ , where  $h = b - d$  is the depth of the canyon) and the dimensionless frequency  $\eta = 0.25, 0.5, 1$  and  $1.5$ . The dimensionless frequency  $\eta$  is defined as the ratio between the width of the canyon and the wave length of the shear waves in the half-space, i.e.  $\eta = 2a/\beta T$  where  $T = 2\pi/\omega$  is the period of the incident waves. In Fig. 6 the canyon is semi-circular and the frequency  $\eta = 2$ .

The analysis of the results showed that the displacement amplitudes on the bottom of the canyon are, in general, smaller for deeper than for shallower canyons. This can be explained by the decrease of the free-field displacement amplitudes with increasing depth. This phenomenon is more pronounced for higher frequencies when the decrease with depth is more rapid. The phases change more rapidly with increasing frequency of the excitation and jumps are noticed at the points where the displacement amplitudes have local minima.

The quality of the results depends on the value of  $N$ , which is the highest index in the truncated infinite series and also on the highest index in the finite Fourier series representing the stresses of the free-field motion. This is especially the case for higher values of  $\eta$ , when the rate of decay of the free-field motion is higher. Since the finite Fourier series in equations (13a,b) represent exactly the stresses at  $2N$  equally spaced points on the circle  $r_1 = b$  and deviate from the exact value of those at the points in between, it is important that  $N$  is chosen such that the points on the rim of the canyon ( $x = \pm a$ ) belong or are close to points of this set. This condition being satisfied, the convergence of the series representing the scattered waves is faster. For example, for  $\eta = 1.5$  and  $h/b = 0.5$  even for  $N = 12$  the error due to the truncation can be neglected.

The biggest advantage of this method, relative to the presently available numerical methods for treatment of the same class of problems, is that it requires simultaneous solution of much smaller system of equations. This may increase the upper frequency limit of its applicability and make it more desirable when the response in the time domain is sought. A disadvantage is that in the form presented in this paper the method can be used only for cylindrical canyons. However, because of the flexibility of the depth-to-half-width ratio and the gradually decreasing depth near the rims, this model may be used for analysis of realistic shallow canyons. Also, the method can be generalized for irregular shape canyons, as discussed in Todorovska and Lee (1991a) and Mocen-Vasiri and Trifunac (1988a,b).



## SUMMARY AND CONCLUSIONS

A new analytical method, previously applied to canyons for incident plane monochromatic SH, P and SV-waves, was extended here to analyse the scattering of monochromatic Rayleigh waves from circular two-dimensional canyons. The shape of the canyons can vary from shallow to semi-circular. Finite Fourier series were used to approximate the stresses of the free-field motion along the bottom of the canyon and infinite Fourier-Bessel series to represent the scattered waves. The analysis of the results showed that displacement amplitudes and phases depend strongly on the frequency of the excitation as well as on the depth of the canyon. This method can be further generalised for irregular shape canyons. The advantage of this analytical method to the presently available numerical methods is that it requires solution of much smaller simultaneous systems of equations, which will increase the frequency limit of its applicability.

## REFERENCES

1. Cao, H. and V.W. Lee (1989). "Scattering of Plane SH Waves by Circular Cylindrical Canyons of Various Depth-to-Width Ratios," *European J. of Earthquake Engineering*, Vol. III - n.2, 29-37.
2. Cao, H. and V.W. Lee (1990). "Scattering of Plane P Waves by Circular Cylindrical Canyons with Various Depth-to-Width Ratios," *Int. J. of Soil Dynamics and Earthquake Engineering*, Vol. 9, No. 3, 141-150.
3. Eringen, A.C. and E.S. Suhubi (1975). "Elastodynamics", Volume II, Academic Press, New York.
4. Kojić, S., M.D. Trifunac and V.W. Lee (1988). "Earthquake Response of Arch Dams to Nonuniform Canyon Motion," Dept. of Civil Eng. Report No. 88-03, University of Southern California, Los Angeles, California.
5. Lee, V.W. (1982). "A Note on Scattering of Elastic Plane Waves by a Hemi-Spherical Canyon," *Int. J. of Soil Dynamics and Earthquake Engineering*, Vol. 1, 122-129.
6. Lee, V.W. and H. Cao (1989). "Diffraction of Plane SV Waves by Circular Canyons of Various Depths," *ASCE, Engineering Mechanics Division*, Vol. 115, No. 9, 2035-2056.
7. Moeen-Vaziri, N. and M.D. Trifunac (1988a) "Scattering and Diffraction of Plane SH Waves by Two-Dimensional Inhomogeneities," *Int. J. Soil Dynamics and Earthquake Engineering*, Vol. 7, No. 4, 179-188.

8. Moeen-Vaziri, N. and M.D. Trifunac (1988b) "Scattering and Diffraction of Plane P Waves and SV Waves by Two-Dimensional Inhomogeneities," *Int. J. Soil Dynamics and Earthquake Engineering*, Vol. 7, No. 4, 189-200.
9. Sánchez-Sesma, F.J. (1987). "Site Effects of Strong Ground Motion," *Int. J. of Soil Dynamics and Earthquake Engineering*, Vol. 6, No.2.
10. Todorovska, M.I. and V.W. Lee (1991a). "Surface Motion of Shallow Circular Cylindrical Valleys for Incident Plane SH Waves-Analytical Solution," *Int. J. of Soil Dynamics and Earthquake Engineering* (in press).
11. Todorovska, M.I. and V.W. Lee (1991b). "Surface Motion of Circular Alluvial Valleys of Variable Depth for Incident Plane SV-Waves Analytical Solution," *Int. J. of Soil Dynamics and Earthquake Engineering* (accepted for publication).
12. Trifunac, M.D. (1971). "A Method for Synthesizing Realistic Strong Gound Motion", *Bull Seism. Soc. Amer.*, Vol. 61 No. 6, 1739-1753.
13. Trifunac, M.D. (1973). "Scattering of Plane SH Waves by a Semi-Circular Canyon," *Earthquake Engineering and Structural Dynamics*, Vol. 1, 267-281.
14. Wong, H.L. (1979). "Diffraction of P, SV and Rayleigh Waves by Surface Topographies", U.S.C. Report No. CE 79-05, Los Angeles, CA 90080-114.
15. Wong, H.L. and M.D. Trifunac (1974). "Scattering of Plane SH Wave by a Semi-Elllyptical Canyon," *Earthquake Engineering and Structural Dynamics*, Vol. 3, 157-169.

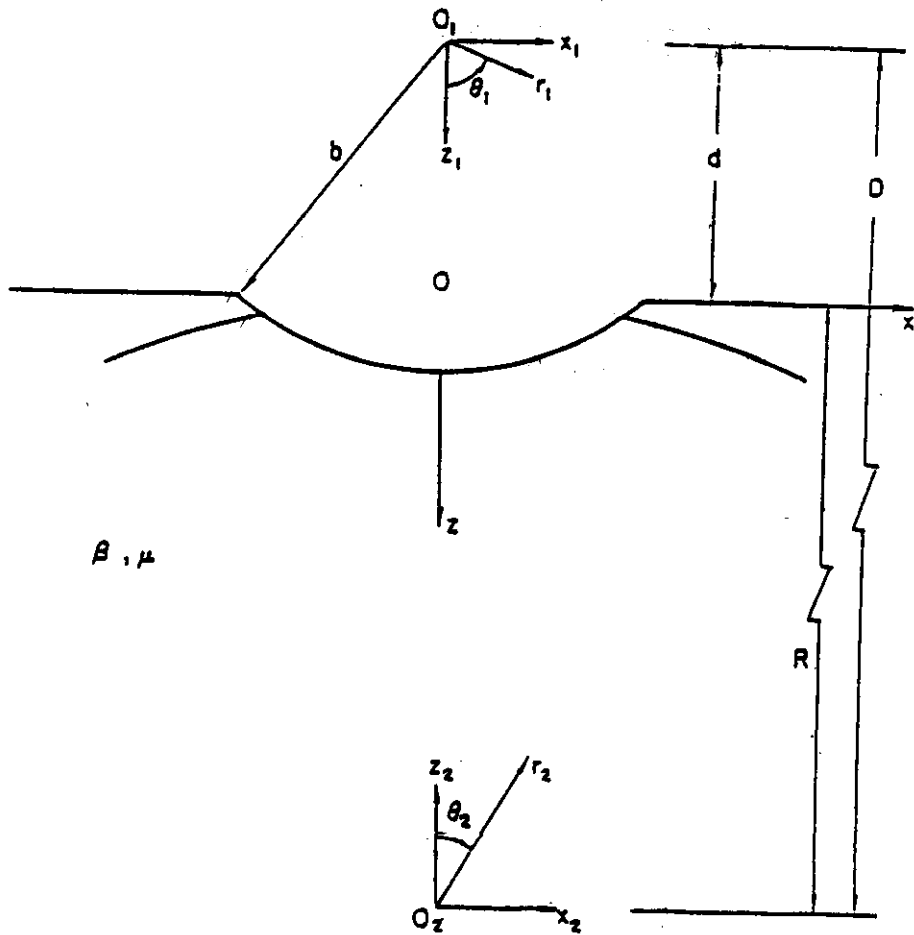


Figure 1 A shallow circular cylindrical canyon in the homogeneous elastic half-space.

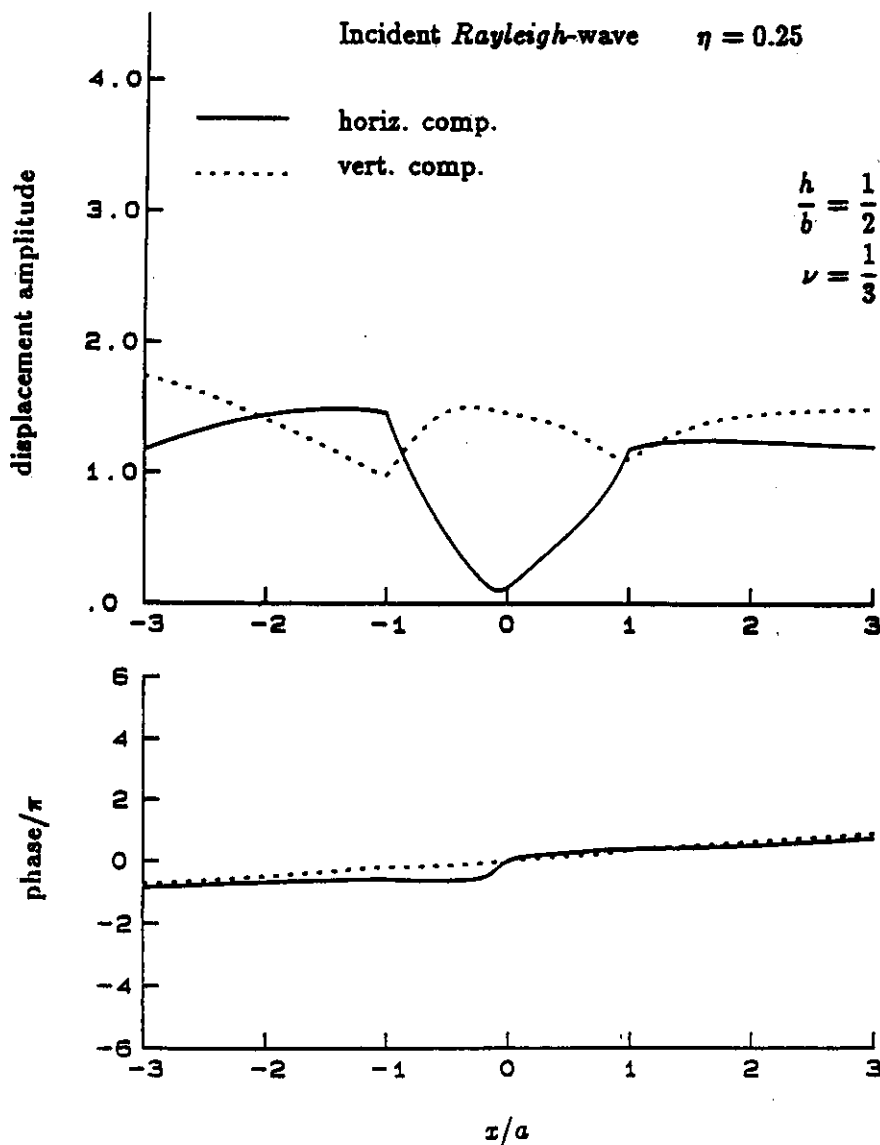


Figure 2 The amplitudes and phases of the horizontal and vertical displacement components on the surface of the canyon ( $-1 \leq x/a \leq 1$ ) and of the half-space ( $x/a < -1$  and  $x/a > 1$ ) versus the distance  $x/a$ . The excitation is a Rayleigh wave with unit amplitude of the horizontal displacement component and dimensionless frequency  $\eta = 0.25$ . The assumed Poisson's ratio is  $\nu = 1/3$  and the ratio between the depth of the canyon and its radius of curvature is  $h/b = 1/2$ .

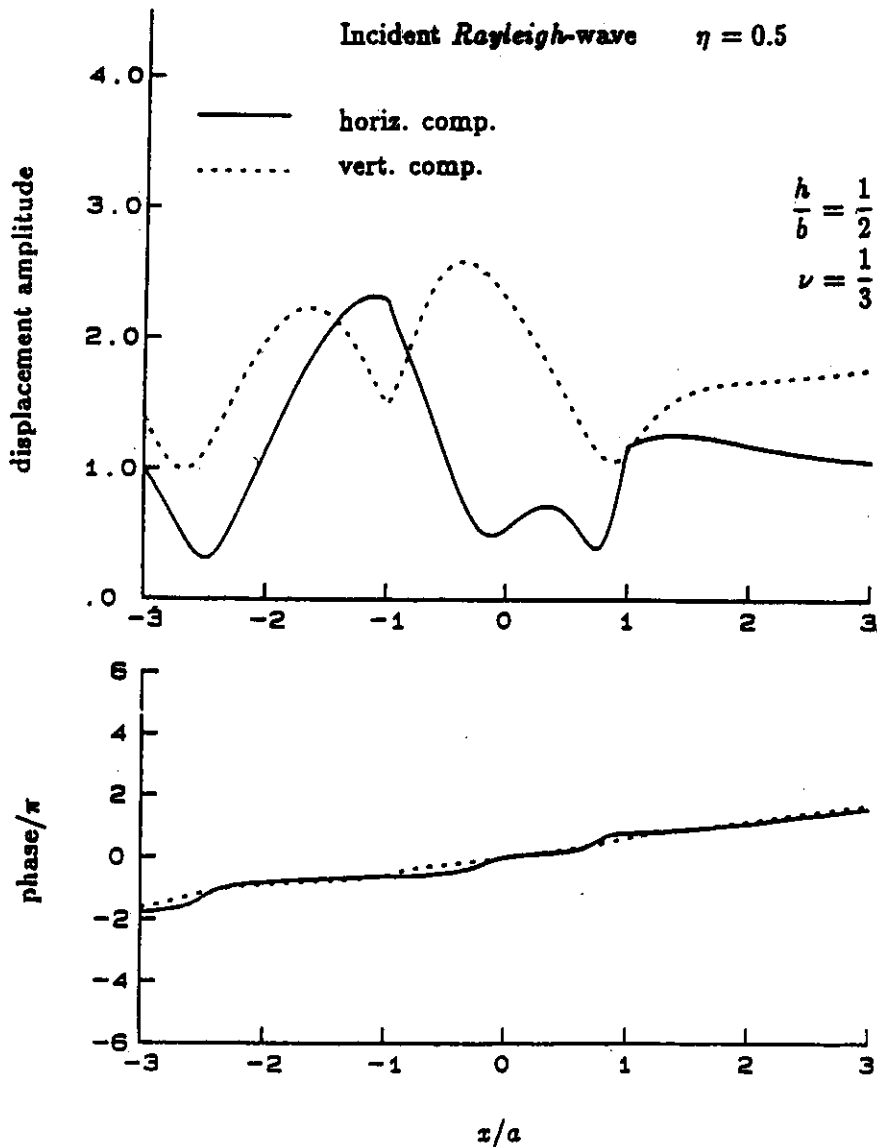


Figure 3 The amplitudes and phases of the horizontal and vertical displacement components on the surface of the canyon ( $-1 \leq x/a \leq 1$ ) and of the half-space ( $x/a < -1$  and  $x/a > 1$ ) versus the distance  $x/a$ . The excitation is a Rayleigh wave with unit amplitude of the horizontal displacement component and dimensionless frequency  $\eta = 0.5$ . The assumed Poisson's ratio is  $\nu = 1/3$  and the ratio between the depth of the canyon and its radius of curvature is  $h/b = 1/2$ .

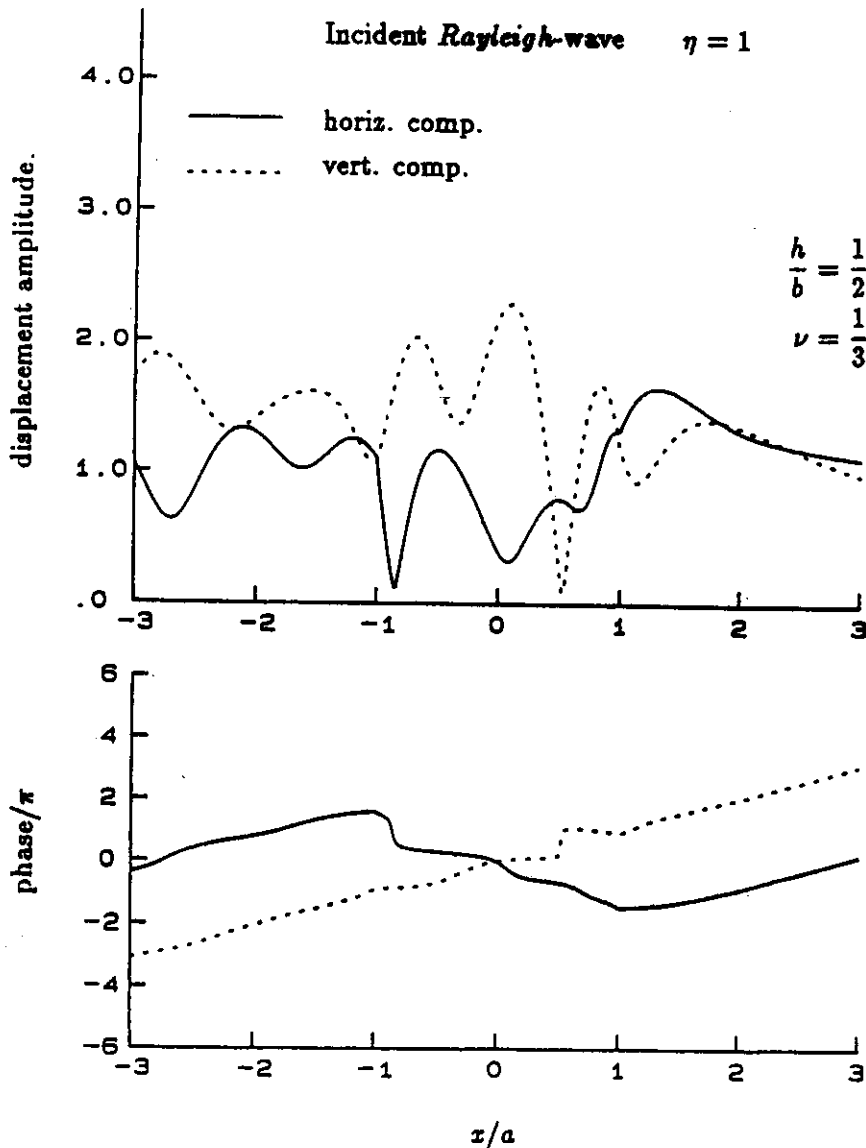


Figure 4 The amplitudes and phases of the horizontal and vertical displacement components on the surface of the canyon ( $-1 \leq x/a \leq 1$ ) and of the half-space ( $x/a < -1$  and  $x/a > 1$ ) versus the distance  $x/a$ . The excitation is a Rayleigh wave with unit amplitude of the horizontal displacement component and dimensionless frequency  $\eta = 1$ . The assumed Poisson's ratio is  $\nu = 1/3$  and the ratio between the depth of the canyon and its radius of curvature is  $h/b = 1/2$ .

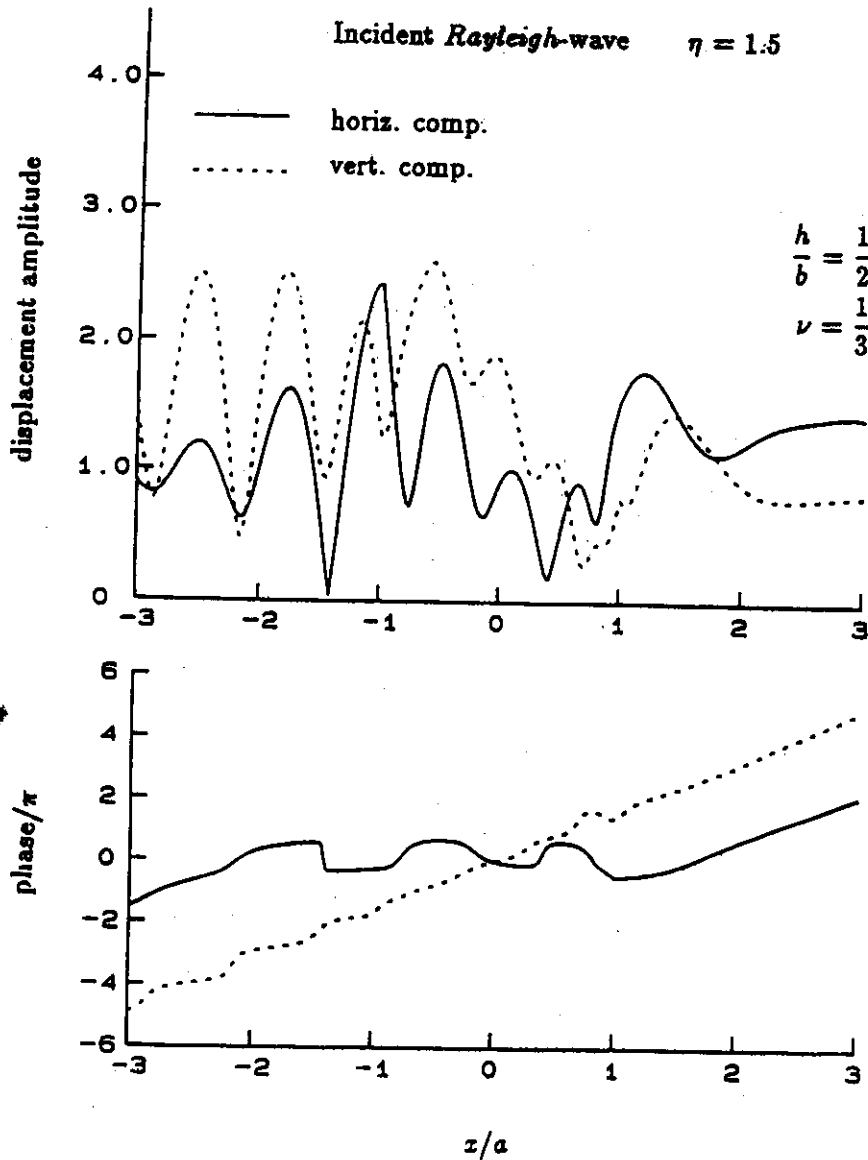


Figure 5 The amplitudes and phases of the horizontal and vertical displacement components on the surface of the canyon ( $-1 \leq x/a \leq 1$ ) and of the half-space ( $x/a < -1$  and  $x/a > 1$ ) versus the distance  $x/a$ . The excitation is a Rayleigh wave with unit amplitude of the horizontal displacement component and dimensionless frequency  $\eta = 1.5$ . The assumed Poisson's ratio is  $\nu = 1/3$  and the ratio between the depth of the canyon and its radius of curvature is  $h/b = 1/2$ .

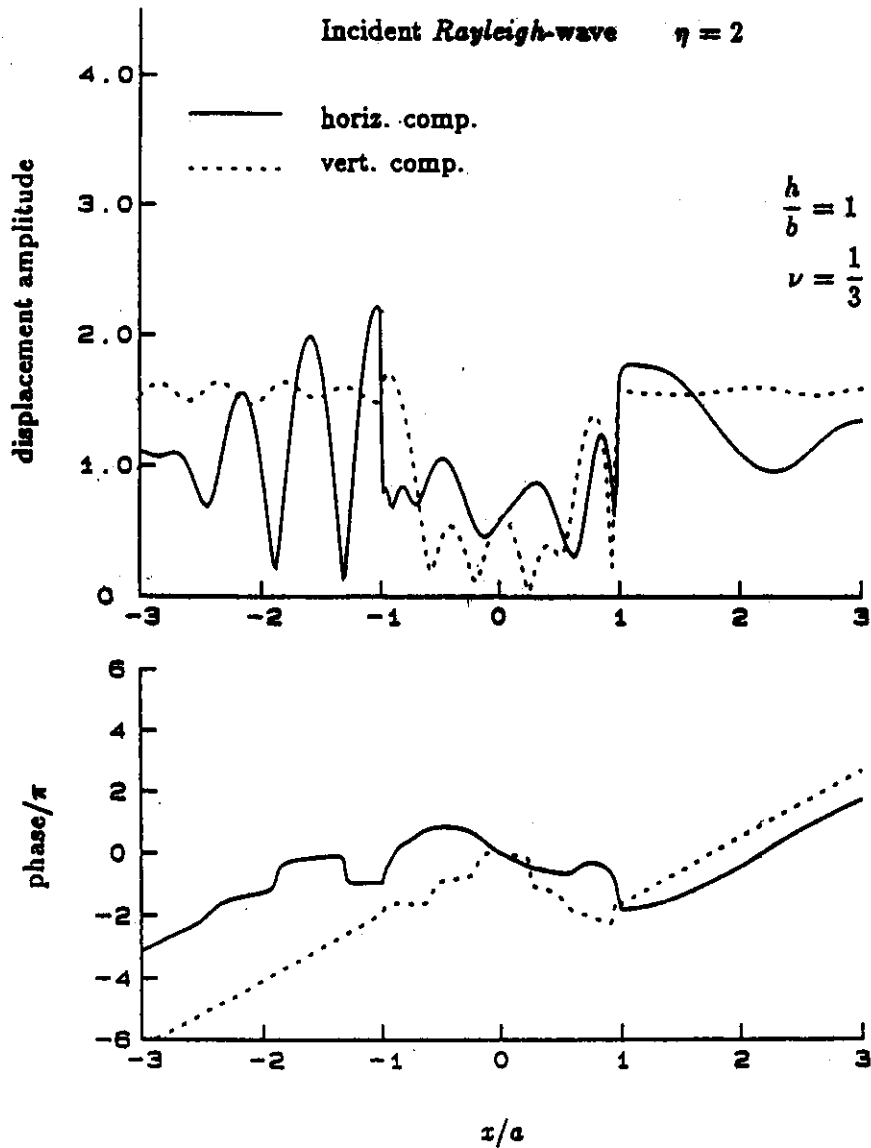


Figure 6 The amplitudes and phases of the horizontal and vertical displacement components on the surface of the canyon ( $-1 \leq x/a \leq 1$ ) and of the half-space ( $x/a < -1$  and  $x/a > 1$ ) versus the distance  $x/a$ . The excitation is a Rayleigh wave with unit amplitude of the horizontal displacement component and dimensionless frequency  $\eta = 2$ . The assumed Poisson's ratio is  $\nu = 1/3$  and the ratio between the depth of the canyon and its radius of curvature is  $h/b = 1$ .